1996ApJ...456L..63T

THE ASTROPHYSICAL JOURNAL, 456:L63–L65, 1996 January 1
© 1996. The American Astronomical Society. All rights reserved. Printed in U.S.A.

INTERACTING ACTIVE REGIONS IN THE SOLAR CORONA

SAKU TSUNETA
Institute of Astronomy, The University of Tokyo, Mitaka, Tokyo 181
Received 1995 August 17; accepted 1995 October 13

ABSTRACT

We report an episode from the *Yohkoh* soft X-ray observations during which antiparallel coronal magnetic fields from two separate active regions, located in opposite hemispheres, reconnect and form new transequatorial coronal loops. Strong evidence for magnetic reconnection consists of the following: (1) Transequatorial connections not previously observed are newly created, (2) an X-point and separatrix structure are clearly seen in the soft X-ray images, and (3) the plasma temperature of the downstream side of reconnection is ~4–7 MK, whereas that of the upstream side is ~2 MK. The quiet coronal plasma is significantly heated over a few days, and the overall magnetic structure of the region is completely changed as a result of magnetic reconnection. This observation suggests that magnetic reconnection occurs also in the quiet corona in a less explosive way than in solar flares and that it may contribute to the overall heating of the quiet corona.

Subject headings: MHD — Sun: activity — Sun: corona — Sun: magnetic fields

1. INTRODUCTION

Magnetic field line reconnection (annihilation of antiparallel magnetic fields) is believed to serve as a highly efficient engine to convert magnetic energy into plasma kinetic and thermal energies in solar, astrophysical, and magnetospheric plasmas (e.g., Petschek 1964; Priest & Forbes 1986). Its actual occurrence in the solar corona, however, has not been confirmed by observations and has been doubted by some investigators because of a theoretical difficulty (a large magnetic Reynolds number of $\sim 10^{12}$). Recent observations with *Yohkoh* X-ray telescopes (Ogawara et al. 1991, and references therein) verify this theoretical prediction for solar flares (Tsuneta et al. 1992; Tsuneta 1996; Masuda et al. 1994; Shibata et al. 1995).

This Letter presents observations that magnetic reconnection also plays a key physical role in the restructuring of the quiet-Sun magnetic field and the heating of the quiet-Sun plasma: the antiparallel coronal magnetic fields from two separate active regions, located in opposite hemispheres, reconnect, and new transequatorial coronal loops are formed. Since the toroidal magnetic fields embedded at the bottom of the convection zone are believed to emerge to the surface of the Sun to form active regions separately and independently in the northern and southern hemispheres (e.g., Harvey 1993; Howard 1994; Moreno-Insertis 1986), the transequatorial loops must be produced in the corona rather than coming directly through the convection zone. Thus, the very existence of the significant transequatorial X-ray loop structure reported here provides basic evidence for coronal reconnection. Transequatorial loops were first discovered in the *Skylab* observations (Svestka, Krieger, & Chase 1977; Sheeley et al. 1974; Sakurai & Uchida 1977). The present observation shows in detail how the interconnecting loops are formed by magnetic reconnection.

Although the reconnection itself is a local phenomena around an X-point, it involves a global reconfiguration of the northern and southern coronal magnetic fields and heats a quiet-Sun plasma of large area. The newly formed coronal connection of the northern and southern toroidal fields, if significant, may also be important for the solar dynamo problem. The implications for the heating of the quiet corona and the behavior of the subsurface magnetic fields are also discussed.

2. OBSERVATION

2.1. *X-Ray Morphology*

Two active regions (NOAA 7116 [southern hemisphere] and 7117 [northern hemisphere]) appeared on either side of the equator on the east solar limb on around 1992 March 23. Figure 1*d* (Plate L6) shows the longitudinal component of the photospheric magnetic fields observed at the US National Solar Observatory/Kitt Peak when they were located near the center of the Sun on 1992 March 30. The corresponding polarities of the two regions are reversed, following Hale's law (e.g., Stix 1991, p. 301), and the distribution of the magnetic fields is symmetric in position about the equator. Figure 1*a* shows a corresponding *Yohkoh* soft X-ray image. In addition to the closed field lines within the active regions, we see an X-shaped structure and loops connecting the two active regions over the equator. The four magnetic poles on the photosphere produce a quadrupolar magnetic structure in the corona, and the X-shaped structure in the soft X-ray image reflects this.

Figure 2 (Plate L7) shows the evolution of the regions from their appearance on the east limb to their disappearance on the west limb. When they appear on the east limb on 1992 May 23, the X-ray structure connecting the northern and the southern active regions is hardly seen; both of the active regions appear self-contained. The X-shaped structure can be seen in data starting on March 24 and remains until about March 30. (It is not clear whether the appearance and disappearance of the X-structure occur on those dates or are due to the projection effect resulting from solar rotation.) The number of X-ray loops connecting the two regions increases in time. When they are near the center of the Sun on March 28 and 29, a rich bundle of X-ray loops connecting the two regions is clearly seen.

Figure 3 (Plate L8) shows X-ray images of the east and west limbs when the regions are located near the limb. The long-exposure (2.7 s) image taken at 0233 UT on 1992 May 23 does not show clear structure connecting the two regions,

© American Astronomical Society • Provided by the NASA Astrophysics Data System

1996ApJ...456L..63T

whereas even the shorter exposure (0.47 s) images taken at 1136 and 1911 UT on 1992 April 4 show loop structures connecting the two regions. These frames show that the region between the two active regions is brighter than the usual quiet Sun, implying the existence of a rich bundle of the magnetic flux tubes between the active regions.

As the regions reach the west limb from the center, transient brightenings of slender transequatorial loops (e.g., 2150 UT on April 2 in Fig. 2 and 0010 UT on April 4 in Fig. 3) and remarkable flarelike cusp structures (e.g., 0034 UT on April 1 in Fig. 2) connecting the two regions are observed. These transient heatings appear not to be directly related to reconnection at the X-point. Rather, these transient brightenings and the cusp structures are similar to those seen in the active regions (Shimizu et al. 1992, 1994; Yoshida & Tsuneta 1996; Tsuneta 1996; Tsuneta et al. 1992). This indicates that the two active regions together form a larger active area, and a separate reconnection process may occur, such as active region brightening.

2.2. *Temperature Structure*

We obtained a temperature map (Fig. 1*b*) of the region from a pair of X-ray images taken with different broadband filters: thin aluminum and Al/Mg/Mn composite filters. This particular combination of the filters is sensitive to temperature below 9 MK. We assume isothermality for the temperature analysis. Since a single X-ray image does not have enough photons for the temperature analysis of the quiet Sun, we sum ~40 full-Sun images for each filter over 15 hr (0–15 UT, 1992 March 28) after correcting for spacecraft jitter and rotation of the Sun. In the long-exposure images, the saturated electrons of the south active region bleed to the quiet Sun along the CCD vertical columns. We do not include the resulting saturated pixels, and we use only the data from the shorter exposure images for those corrupted pixels.

Although the basic X-shaped structure persisted during the integration time of 15 hr, there were some variations in X-ray morphology and brightness, especially on the downstream side of reconnection site. In the observing sequence, images with the thin aluminum and Al/Mg/Mn composite filters are taken alternately, and time variations with timescales longer than 11 minutes (the average interval) are thus reduced in the temperature map. We thus obtain "time-averaged" temperatures. Time variation with shorter timescales, however, can potentially produce errors in the derived temperatures. Since the new bundle of loops to the east and west of the reconnection site (X-point) appears to have more transient phenomena, the temperature analysis is restricted to the region close to the X-point.

Figure 1*b* shows an X-shaped structure in the temperature map as well. In the temperature map, four different sectors are separated by the magnetic separatrix lines, east and west sectors and north and south sectors facing each active region. The temperature of the east and the west sectors is ~4–7 MK, whereas the temperature of the north and the south sectors is significantly lower and is ~2–3 MK. (The active region temperatures are generally 3–8 MK [Yoshida & Tsuneta 1996].) The north and south sectors have much lower temperatures (except in the active regions) and are thus identified as the upstream sides of the reconnection region. (Fig. 2*b* shows that a few loops in the upstream [located in between the X-point and the south active region] have somewhat higher temperatures, but the upstream side essentially has lower temperature than the downstream side.) The high-temperature regions spread over a few 10^5 km near the X-point and are separated to the lower temperatures of the upstream by the separatrices seen in the X-ray images.

3. DISCUSSION AND CONCLUSION

3.1. *Magnetic Reconnection*

We now have some strong evidence that magnetic reconnection is responsible for the formation of the transequatorial field lines in the active regions NOAA 7116 and 7117: (1) Transequatorial connections not previously observed are newly created. (2) An X-shaped structure is clearly seen between the two active regions. (3) The number of X-ray loops connecting the two active regions increases during the disk passage. (4) The temperature of the downstream side of the reconnection is ~4–7 MK, while that of the upstream side is ~2–3 MK.

Some of the transequatorial structures have distinct (isolated) bright loops. This implies that magnetic reconnection occurs intermittently and produces these isolated flux tubes as a result. Figure 2 also shows that the bright transequatorial loops are located somewhat away from the central reconnection site. This may be due to the evaporation time lag. Since the length of the reconnected loops is about $l = 10^5$ km or more, the timescale for the evaporated plasmas to fill the interconnecting loops is $\sim l/v_s \sim 384$ s after the start of the energy injection (reconnection), where $v_s \sim 260$ km s^{-1} is sound velocity for $T = 5 \times 10^6$ K. This timescale is much longer than the Alfvén transit time $d/v_A \sim 50$ s for the east-west length of the high-temperature region $d \sim 5 \times 10^4$ km and the coronal Alfvén speed $v_A \sim 10^3$ km s^{-1}. Since the velocity of the downstream outflow plasma is close to the Alfvén velocity of the upstream side (e.g., Petschek 1964), the reconnected loops become more visible in X-rays after their traverse across the downstream high-temperature region. This evaporation time lag may explain the observations that the transequatorial loops are seen somewhat away from the X-point (to the east and west sides of the downstream).

Uchida et al. (1992) discovered that the closed field lines in active regions sometimes expand on the limb with speed of a few to a few times 10 km s^{-1}. We assume that the same expansion occurs in these active regions, drives reconnection, and supplies the magnetic flux to the reconnection site. The expansion speed of the active region fields would then govern the overall speed of reconnection. For a typical inflow speed from the active regions of 10 km s^{-1}, the Alfvén Mach number is $M_A \sim 0.01$ for a typical coronal Alfvén speed of 1000 km s^{-1}. This implies that the upstream field lines are almost antiparallel and that the acute half-angle of the separatrix lines is as small as $M_A^{-1}/2 \sim 0.^\circ3$ in the incompressible case (Petschek 1964; Parker 1979, p. 420). Viewed from the active regions (upstream side), however, the observed angle of the separatrices is ~90° or less than 90°. In order to have magnetic reconnection occur, the angle must be greater than 90°. Magnetic fields close to the reconnection site may be almost antiparallel because of the pressed loops from the two active regions. These separatrix lines are connected to the global separatrix lines (due to the quadrupolar magnetic structure) seen in the X-ray images. An alternative explanation is the nonuniform reconnection model proposed by Priest & Lee (1990). Petschek theory treats uniform magnetic fields in the

© American Astronomical Society • Provided by the NASA Astrophysics Data System

1996ApJ...456L..63T

inflow, with the small curvature of the field lines as a linear perturbation. Priest & Lee found a fast steady state solution possessing highly curved magnetic field lines.

3.2. *Implication for the Quiet-Sun Coronal Heating*

High temperatures would be created along the loops that spread far from the reconnection site partly by the high thermal conductivity along the reconnected magnetic fields, partly by a fast outflow at the Alfvén velocity, and partly by the effect of the reconnection shock wave. The conductive timescale of the downstream plasma is given by

$$t_{\rm cond} = \frac{3nkTl}{\kappa_0 T^{5/2}(T/l)}, \quad (1)$$

where $\kappa_0 T^{5/2}$ is the Spitzer thermal conductivity ($\kappa_0 = 10^{-6}$ ergs s^{-1} cm^{-1} K$^{-3.5}$), and l is the scale length of the reconnected loop. The observed emission measure of the downstream is $\sim 10^{27}$ cm^{-5}. If we assume that line-of-sight thickness is 4×10^4 km, the plasma density is $n = 6 \times 10^8$ cm^{-3}. The conduction timescale $t_{\rm cond}$ is then $\sim$450 s for $T = 5 \times 10^6$ K and $l = 10^5$ km. The radiative timescale is

$$t_{\rm rad} = \frac{3nkT}{\Lambda(T)n^2}, \quad (2)$$

where k is the Boltzmann constant and $\Lambda(T)$ is the radiative loss function. Since the temperature T is 5 MK, and the radiative loss function is $\Lambda(T) = 3 \times 10^{-20} T^{-0.5} \sim 2.4 \times 10^{-23}$ ergs s^{-1} cm^{-3}, the radiative cooling time $t_{\rm rad}$ is 10^5 s. The dominant conductive loss is supplied by magnetic reconnection. If the upstream magnetic field $\boldsymbol{B}$ close to the reconnection site is almost antiparallel, most of the magnetic energy fed to the reconnection site is consumed for the eventual heating of the downstream plasma. The conduction energy loss of the downstream plasma is, then, balanced with the energy input from the upstream in the steady state:

$$\frac{\boldsymbol{B}^2}{8\pi} v s_{\rm up} \sim \frac{\kappa_0 T^{3.5}}{l} s_{\rm down}, \quad (3)$$

where v is the inflow speed, $s_{\rm up}$ is the cross-sectional area of the upstream flow, and $s_{\rm down}$ is the cross-sectional area of the reconnected flux tubes. If we assume that v is 10–20 km s^{-1} (Uchida et al. 1992), and $s_{\rm up} \sim s_{\rm down}$ from the X-ray images, we obtain $\boldsymbol{B} \sim$ 27–18 G. Thus, reconnection of expanding active region fields with magnetic field strength of a few times 10 G can heat the plasma to several megakelvins over the area of $\sim 10^5$ km as long as expansion of the active regions continues with speed of a few times 10 km s^{-1}.

Note that the heating over a wide area to such a temperature occurs as a result of single-point reconnection of the two separate macroscopic magnetic structures in the solar corona. Configurations similar to this, although not necessarily so symmetric, may frequently occur in the corona. Active regions appearing on opposite hemispheres inherently have oppositely directed field lines above the equator owing to Hale's law, and the antiparallel fields lines naturally meet there. Reconnection can also occur between nearby active regions in the same hemisphere. Single-point reconnection can heat the plasma over a much larger area in between the active regions, and the conjecture here is that the quiet corona outside active regions is (quasi-)continuously heated as a result of the frequent reconnection of expanding active-region fields. How significant the heating is in terms of the overall heating of the quiet Sun depends on how ubiquitous the active region expansion is.

3.3. *Implication for the Behavior of Toroidal Magnetic Fields*

Reconnection may proceed until the transequatorial loop flux reaches a flux comparable to that of the outer active regions. The two regions become much more intimately connected during their disk passage. Indeed, Figure 3 shows that the X-ray intensity of the region between the two active regions can be as bright as the outer parts of the active regions. This implies that the transequatorial loops contain a considerable part of the magnetic flux from the active regions. The coronal reconnection links the oppositely directed toroidal magnetic fields embedded in the convection zone at the equatorial region and may create isolated toroidal structures separated from the main flux tubes. A long-standing problem in the solar dynamo models has been how to expel the amplified toroidal flux in the solar cycle (Parker 1984; Wang, Sheeley, & Nash 1991). Once the toroidal flux tubes are separated from the main flux tubes by coronal reconnection, the isolated toroidal structures may be expelled from the Sun. Since we now know that coronal reconnection occurs as a result of expanding active regions, escape of the toroidal fields is also possible owing to reconnection of active regions on the same hemispheres, as Parker (1984) suggested.

In spite of the large magnetic Reynolds number ($\sim 10^{12}$) of the solar corona, *Yohkoh* has discovered unambiguous examples of magnetic reconnection in flares and in the quiet corona. Magnetic energy conversion through magnetic reconnection is likely to be a common occurrence throughout the cosmos.

The author would like to thank E. Priest for encouragement regarding this work and H. Hudson, R. Moore, and an anonymous referee for comments on the Letter.

REFERENCES

Harvey, K. L. 1993, Ph.D. thesis, Utrecht Univ.
Howard, R. F. 1994, in Solar Active Region Evolution, ed. K. Balasubramanian & G. Simon (San Francisco: ASP), 1
Masuda, S., Kosugi, T., Hara, H., Tsuneta, S., & Ogawara, Y. 1994, Nature, 371, 495
Moreno-Insertis, F. 1986, A&A, 166, 291
Ogawara, Y., Takano, T., Kato, T., Kosugi, T., Tsuneta, S., Watanabe, T., Kondo, I., & Uchida, Y. 1991, Sol. Phys., 136, 1
Parker, E. N. 1979, Cosmical Magnetic Fields (Oxford: Clarendon)
———. 1984, ApJ, 281, 839
Petschek, H. E. 1964, in Proc. AAS–NASA Symp. on Solar Flares, NASA SP-50, 425
Priest, E. R., & Forbes, T. G. 1986, J. Geophys. Res., 91, 5579
Priest, E. R., & Lee, L. C. 1990, J. Plasma Phys., 44, 337
Sakurai, T., & Uchida, Y. 1977, Sol. Phys., 52, 397
Sheeley, N. R., Bohlin, J. D., Brueckner, G. E., Purcell, J. D., Scherrer, V. S., & Tousey, R. 1974, Sol. Phys., 40, 103
Shibata, K., Masuda, S., Shimojo, M., Hara, H., Yokoyama, T., Tsuneta, S., Kosugi, T., & Ogawara, Y. 1995, ApJ, 451, L83
Shimizu, T., Tsuneta, S., Acton, L. W., Lemen, J. R., Ogawara, Y., & Uchida, Y. 1994, ApJ, 422, 906
Shimizu, T., Tsuneta, S., Acton, L. W., Lemen, J. R., & Uchida, Y. 1992, PASJ, 44, L147
Stix, M. 1991, The Sun (Berlin: Springer)
Svestka, Z., Krieger, A. S., & Chase, R. C. 1977, Sol. Phys., 52, 69
Tsuneta, S. 1996, ApJ, 456, 840
Tsuneta, S., Hara, H., Shimizu, T., Acton, L. W., Strong, K. T., Hudson, H. S., & Ogawara, Y. 1992, PASJ, 44, L63
Uchida, Y., McAllister, A., Strong, K. T., Ogawara, Y., Shimizu, T., Matsumoto, R., & Hudson, H. S. 1992, PASJ, 44, L155
Wang, Y. M., Sheeley, N. R., Jr., & Nash, A. G. 1991, ApJ, 383, 431
Yoshida, T., & Tsuneta, S. 1996, ApJ, in press

© American Astronomical Society • Provided by the NASA Astrophysics Data System

1996ApJ...456L..63T

PLATE L6

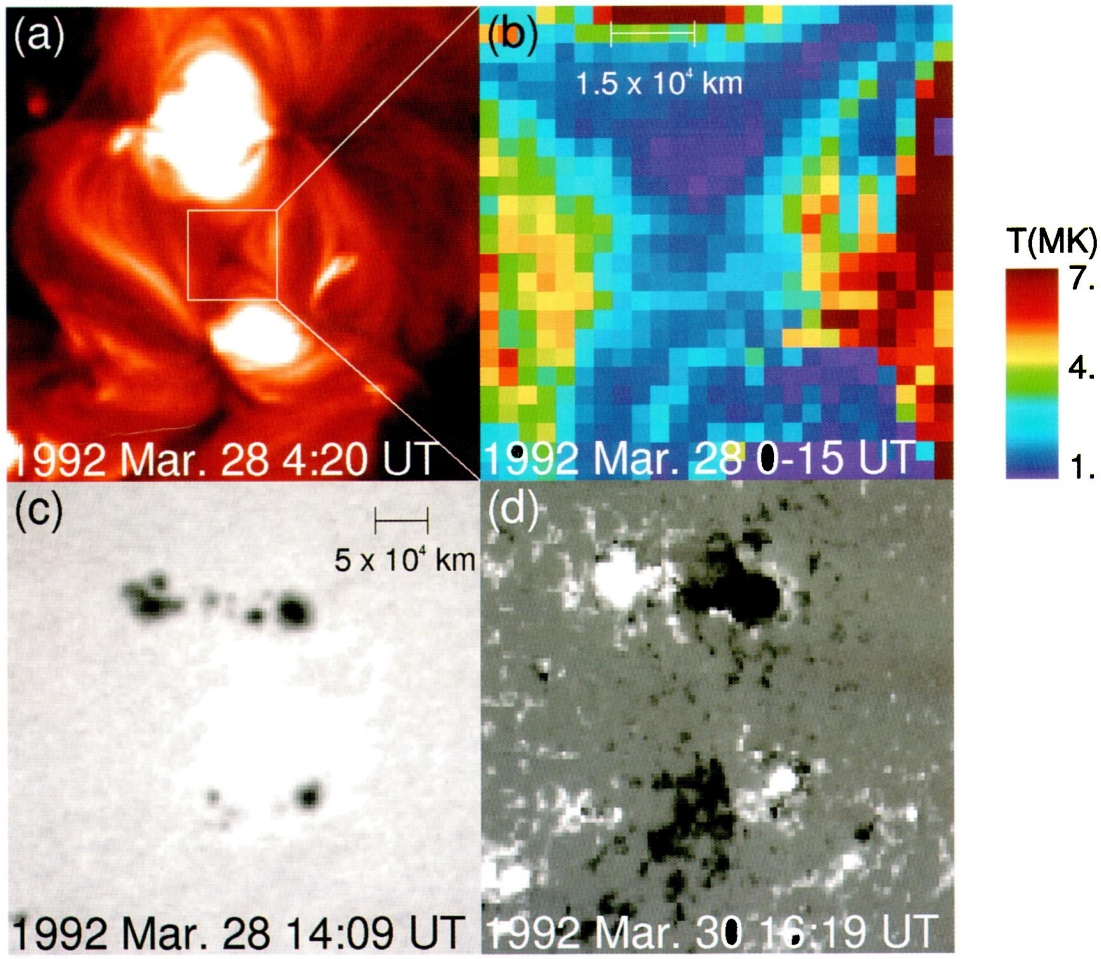

FIG. 1.—(*a*) Soft X-ray image taken with the thin aluminum filter. The pixel size is 4.″9, and the field of view is 10.′5 × 10.′5 (128 × 128 pixels). East is to the left, and north is up. The solar equator is located in between the two active regions. (*b*) Temperature map obtained with a pair of broadband filters (thin aluminum and Al/Mg filter) for the box region of panel (*a*). The pixel size is the same (4.″9), and the field of view is 2′ × 2′ (24 × 24 pixels). Fifteen hours of data (0–15 UT, 1992 March 28; ~40 image data each for two filters) are summed to obtain the temperatures of the region outside the active regions. (*c*) Narrowband optical image taken with *Yohkoh*. (*d*) Longitudinal magnetograph image (National Solar Observatory/Kitt Peak). The gray scale indicates the polarity and the magnitude of the longitudinal magnetic fields.

TSUNETA (see 456, L63)

© American Astronomical Society • Provided by the NASA Astrophysics Data System

© American Astronomical Society • Provided by the NASA Astrophysics Data System

1996ApJ...456L..63T

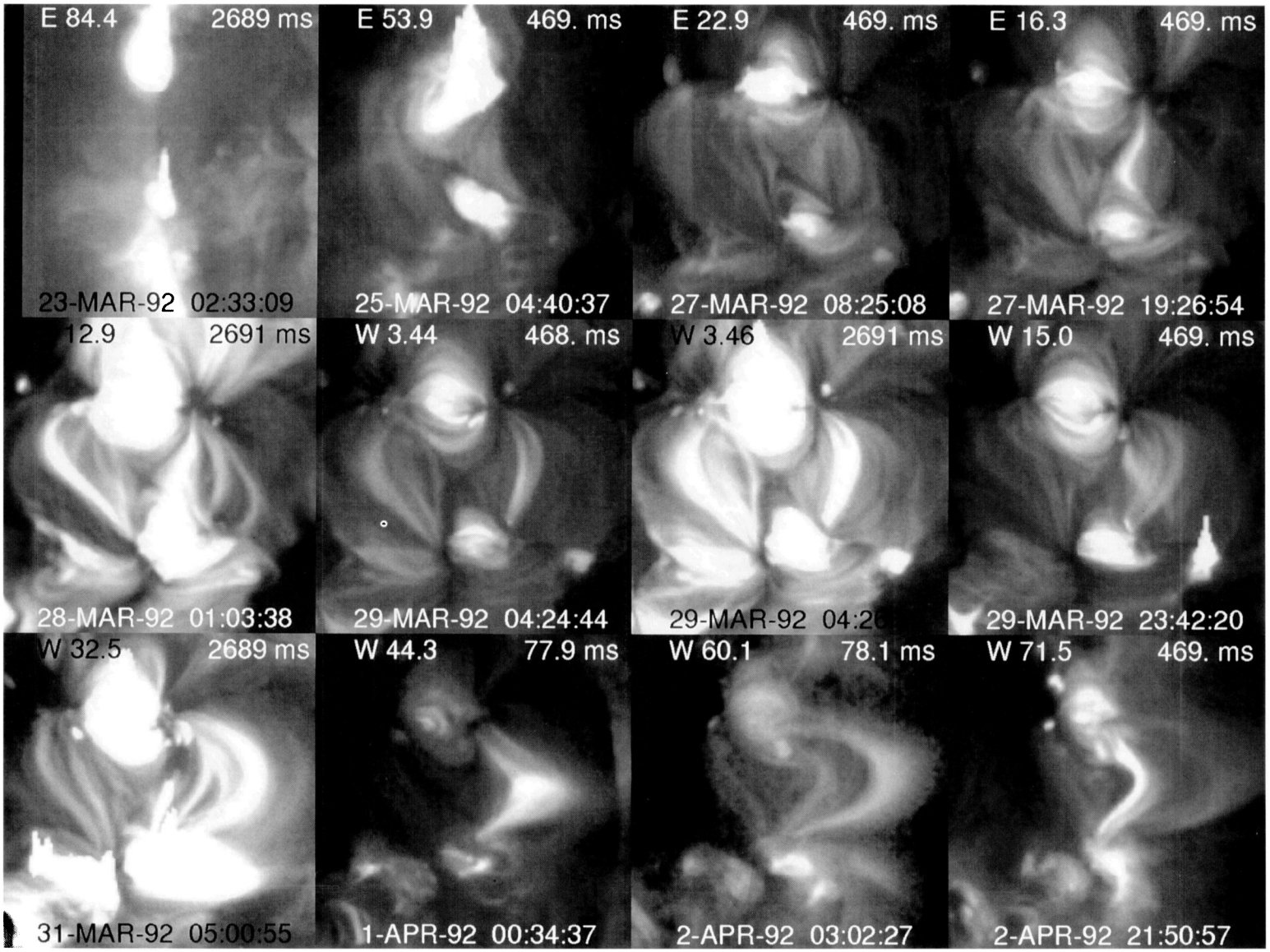

FIG. 2.—The evolution of the interacting active regions from their appearance on the east limb until disappearance on the west limb. The pixel size is 4.″9, and the field of view is 10.′5 × 10.′5 (128 × 128 pixels). East is to the left, and north is up. The number of transequatorial loops increases, and transient activities start to appear in between the active regions as they close to the west limb. The locations of the active regions are indicated on the top left and the exposure times on the top right. The active regions are saturated in the long-exposure images, and the spillover photoelectrons bleed to the north.

TSUNETA (see 456, L63)

1996ApJ...456L..63T

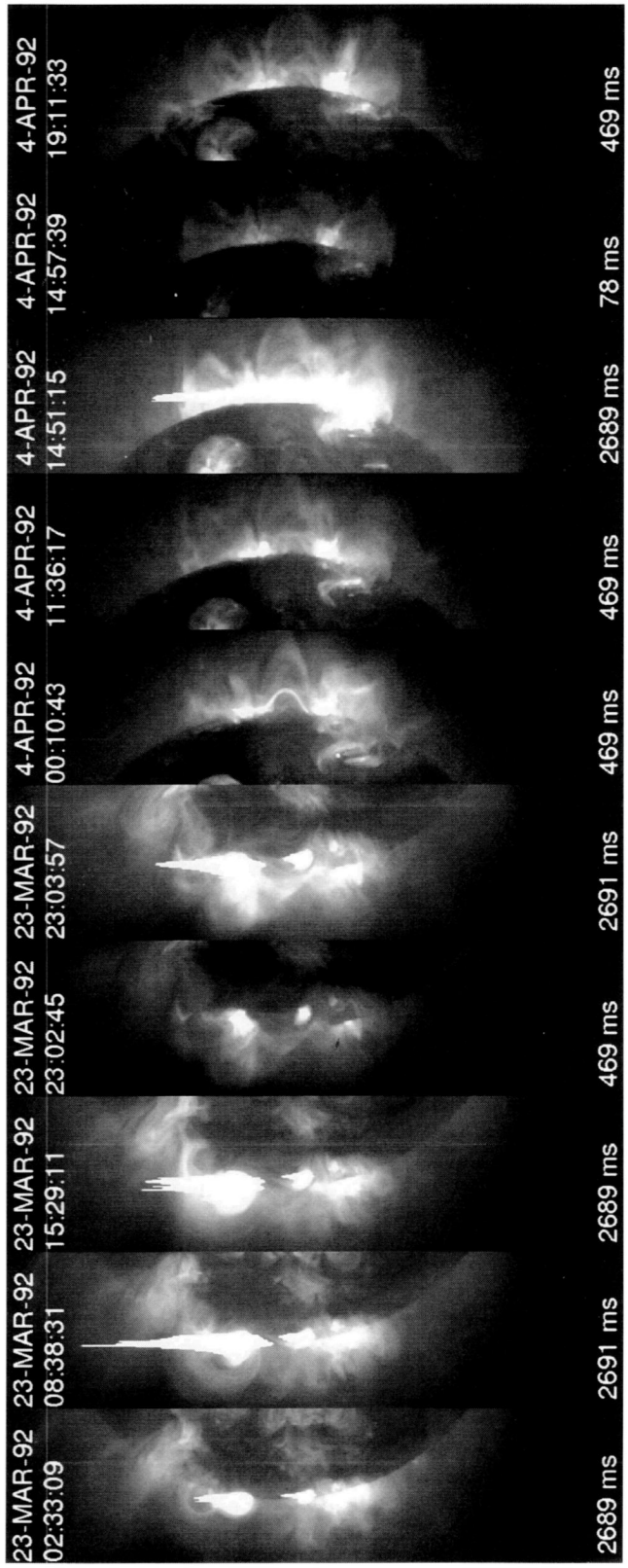

FIG. 3.—The two active regions located on the east and the west limb. The pixel size is 4.″9, and the field of view is 128 (north-south) × 512 (east-west) pixels. East is to the left, and north is up. The comparison of the two images with same exposure time shows the loop structures with increased X-ray intensity in between the two active regions in the west limb picture. The exposure times are indicated at the bottom of the slices. The active regions are saturated in the long-exposure images, and the spillover photoelectrons bleed to the north.

© American Astronomical Society • Provided by the NASA Astrophysics Data System